



Fuzzy Yaw Angle Controller for an Electric Tracked Vehicle

Mohamadreza Satvati¹, Abdollah Amirkhani¹, Seyed Vahid Nourbakhsh borujerd¹, Masoud Masih-Tehrani^{1*}

¹ Vehicle Dynamical System Research Lab, School of Automotive Engineering, Iran University of Science and Technology, Tehran, Iran

ARTICLE INFO

Article history:

Received : 2 Oct 2020

Accepted: 6 June 2021

Published: 1 Dec 2021

Keywords:

Electric tracked vehicle
Trafficability

Yaw angle controller

Slope-traversing

Fuzzy controller

ABSTRACT

This paper experimentally investigates the trafficability of a small tracked vehicle on a slope. An increase in the angle of slope inclination may divert the vehicle from its path. In other words, the deviation of the vehicle is due to a sudden increase in the yaw angle. Also, the tip-over occurs at a specific slope angle. The locomotion of the small tracked vehicle on soils with different terramechanics (such as cohesion, internal friction angle, cohesive modulus, and friction modulus) is also simulated to evaluate its slope-traversing performance. Moreover, the impact of velocity and soil type on traversing a slope is measured. The proposed yaw angle control system is modeled for controlling the yaw angle of the tracked vehicle. This controller is designed through co-simulation. It keeps the tracked vehicle at zero yaw angle to achieve straight locomotion on slopes. It is compared to the PI, PID, and fuzzy controllers. The response of this controller is faster than PI and PID controllers. A Comparison between fuzzy and proposed yaw angle controller yields almost similar responses. The mechanism of the proposed yaw angle controller is also easier to understand. The precision of the controller's performance is measured by simulating over different terrains.

*Corresponding Author

Email Address: masih@iust.ac.ir

<https://doi.org/10.22068/ase.2021.560>

1. Introduction

Tracked vehicles are suitable for locomotion in unstructured environments, where there is a large contact area between tracks and ground. Tracked robots are among the essential and useful types of robots [1]. The development of a vehicle/terrain interaction model is a difficult task. Researchers developed empirical methods for predicting vehicle mobility. Experiments can find empirical relationships in different off-road conditions. These relationships are useful for evaluating terrain trafficability and vehicle locomotion [2]. A tracked vehicle's locomotion system has very complicated Kinematic and dynamic characteristics [3].

Bekker [4] developed experimental techniques, such as bevameter. Terramechanics investigate the effects of soil parameters and the interaction of wheeled or tracked vehicles on various surfaces. Modeling of terrain behaviors, measurement, and characterization of mechanical properties of terrain about vehicle mobility, and the mechanics of vehicle-terrain interactions are included in terramechanics [5]. An experimental slip model for exact kinematics modeling was proposed to find the relationship between the slippage of tracks and two main parameters, namely the radius of the tracking path and speed of the robot. The slip coefficients were regarded as an exponential function of the radius of the path's curvature [1]. Yamauchi et al. [6] proposed a slip model for tracked vehicles based on the force acting on a robot on a slope. The effect of pitch and roll angles on the slip ratio was studied. Based on experimental data, several key terrain parameters were identified. The small track-terrain interaction model was proposed, and an innovative platform of the tracked robot was created. The experimental track segment shear test and plate load test in a bentonite-water mixture were done to offer a new empirical model of saturated soft-plastic soil (SSP) for seafloor tracked vehicles. The tractive performance of a tracked vehicle on extremely soft soil was investigated by a tracked vehicle model, which uses a pair of driving chain links driven by two AC-servo motors [7-9]. Schulte et al. [10] performed an experimental traction test with a track segment in an embedded bed. A series of track experiments were conducted on a modeled track system with silty sand

to investigate a new mechanism for the side thrust. The results showed the shapes of the failure surfaces, and the side thrust was measured for verification purposes [11]. Gallina et al. [12] proposed probabilistic and nonprobabilistic techniques for efficient treatment of soil parameter uncertainties in rover position predictions. Experiments were carried out in the planetary exploration laboratory [12]. Choi et al. [9] investigated the straight driving performance of a tracked vehicle on cohesive soft soil. Small slip and little torque were interpreted as an excellent performance of the vehicle, especially for soft and sensitive surfaces [9]. Schulte et al. [10] performed a stand test, ring shear test, vane test, track segment test, cone tests and plate load tests in the bentonite-water mixture. Ting Zou et al. [13] proposed a control procedure using the backstepping method based on the modified proportional integral derivative (PID) and computed-torque controller. The approach was for the dynamic modeling and motion control of a tracked vehicle on a hard soil terrain [13]. Shouxiang Tang et al. [14] presented a high-fidelity, general, and modular method for lateral dynamics simulation of a high-speed tracked vehicle [14]. A path-tracking control algorithm for a tracked drilling machine was presented, including track-soil interactions dynamical model [15]. Dai et al. [16] designed an adaptive neural-fuzzy interface system control algorithm to achieve a better trajectory tracking control performance for a tracked vehicle moving on the seafloor. Some studies analyzed a three-degree-of-freedom (DOF) dynamic model of the tracked vehicles to investigate their lateral dynamics. The parameters are longitudinal motion, lateral motion, and yaw. Janarthanan et al. [17] developed a 5-DOF dynamic model of a tracked vehicle. The model was comprised of roll and pitch DOF [17]. A trajectory tracking controller based on expected yaw velocity was proposed. Low-speed path following, high-speed path following, and high-speed lateral stability strategies for Truck-trailer combination (TTC) were investigated. The driver model and yaw plane model of TTC to achieve the optimal control performance index was proposed [18-19]. Cai et al. [20] developed a trajectory tracking control system, consisting of a model predictive control unit and an active safety steering control. Jin et al. [21] presented gain-scheduled and robust static output feedback controllers to improve yaw stability

control and handling performance of in-wheel-motor-driven electric vehicles [21]. Babu et al. [3] presented a new stability strategy for determining the instability of a high-speed, unmanned, heavy tracked vehicle during the operation. Jiang et al. [22] investigated the wheel-soil interactions for a lunar exploration through physical model tests and numerical simulations.

Experimental tests can help find challenges facing locomotion on a slope. There is a lack of study into the design of a simple and understandable yaw controller while traversing a slope.

The test platform is explained in Section 2. Trafficability on slope tests is dealt with in Section 3. Computer-aided simulation is done in Section 4. In this study, RecurDyn is used for simulation. The proposed yaw angle controller is addressed in Section 5. Co-simulation between Recudyn and MATLAB Simulink is done for designing the yaw controller. Then, it is compared with PI, PID, and fuzzy yaw angle controllers.

2. Test Platform

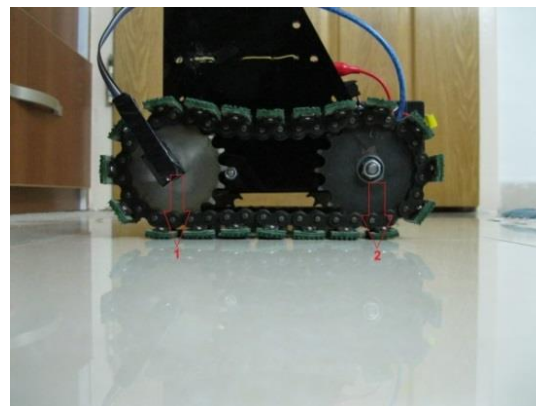
To develop a small laboratory environment and study the dynamic and kinematic phenomena of a motion, a test platform is designed for a small tracked vehicle. This platform includes a small tracked vehicle and a laboratory environment for movement.

2.1. Parameters of Tracked Vehicle Test Platform

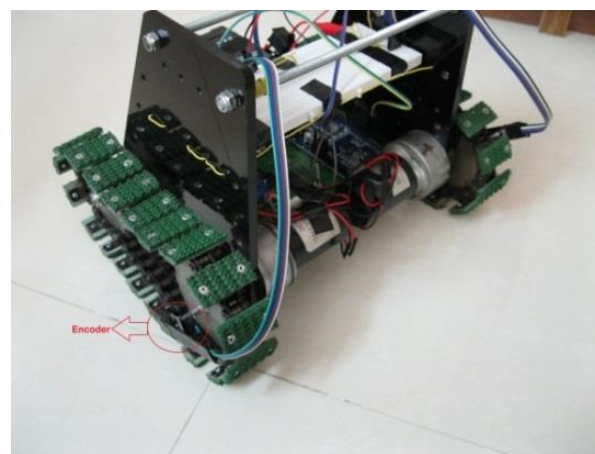
In this research, a small tracked vehicle is used, which includes the main chassis and two-track systems. Each track consists of one sprocket, one idler, and 20 rubber shoes.

Fig. 1 shows the small tracked vehicle's structure and equipment. In this small tracked vehicle, DC motors are connected directly to sprockets. Sprockets are located in the rear of each side of the tracked vehicle. Pose 1 shows the sprocket location in Fig. 1a and Pose 2 shows the idler location in Figure 1a. Both Sprocket and idler are similar in geometry and materials. A chain link is an interface between the sprockets and tracks, as shown in Figure 1a. Due to the complexity of mechanical calculations, it is assumed that sprocket had a direct connection with the track. Energy loss and slip between the chain link

and track are ignored. Table 1 shows the small tracked vehicle and DC motors parameters.



a



b

Fig. 1: The small tracked vehicle structure and equipment: a) track, sprockets, chain link, and idler; b) encoder embedded for obtaining rotational speed of the sprocket

Table 1: The small tracked vehicle and DC motors parameters

Parameter	Value
Max length of the vehicle	22 cm
Max width of the vehicle	27 cm
Max height of the vehicle	22 cm
Weight (total weight with battery and control)	4 kg

equipment)	
Contact track length (for each individual part track)	3.5 cm
Contact track width (for each individual part track)	1.8 cm
The radius of the driving wheel	4.5 cm
Clearance (related to the flat ceramic surface)	3 cm
Tread of the tracked vehicle	24.5 cm
Center of track distance	12.25 cm
Rated DC motor voltage	12 v

2.2 Equipping Tracked Vehicle

The small tracked vehicle is powered by two DC motors (DC MOTOR DME34BE50G-108) and a rechargeable battery (SUNNYBATT, 12 volts). The initial current should be less than 0.87 A. Table 2 shows the battery specifications [23]:

Table 2: Battery specifications

Length	79±1 mm
Width	56±1 mm
Height	99±1 mm
Weight	1.05 kg ± 5%

An Arduino board is used to control the electric motors. Arduino develops the open-source software, and user community that designs and manufactures single-board microcontrollers and microcontrollers kits for building digital devices and interactive objects that can sense and control both physically and digitally [24]. The Arduino software (IDE) allows for programming the board. For working offline, a desktop IDE is used [25]. One of the most critical issues is to preserve the skew-symmetry of the tracked

vehicle. To this end, the rechargeable battery is embedded in the midplane of the foam floor of the tracked vehicle. Although the Arduino board’s weight is negligible to the tracked vehicle, the battery weight is a significant factor to be considered. An encoder is used to measure the speed of the small tracked vehicle. The start speed should be similar in experiments and simulations, and thus, a proper comparison should be made. An encoder is a device, circuit, transducer, software, algorithm, or person that converts information from one format or code to another, for the purpose of standardization, speed or compression [26]. Fig. 1b shows how an encoder was used for obtaining the rotational speed of the sprocket. Another vital component is the driver, which has two important roles. Firstly, it supplies the power required by the Arduino. An Arduino needs 5 volts power to run; therefore, it cannot be directly connected to the battery. The driver is an interface between Arduino and battery. Secondly, Arduino can drive DC motors using the speed control pins.

3. Experimental Trafficability Tests on Slope and Results

First, a speed correction coefficient test is performed to improve the speed reported by the encoder. Then, the experimental slope tests are carried out.

3.1 Slope Traversal Test

In this section, the slope traversability of a small tracked vehicle is studied. The initial slope angle is 13 degrees, which increases throughout the experiments. In each step, the test is done in two modes, once with and once without an arm. The aim was to find the critical slope for hanging up the small tracked vehicle in both styles.

In this test, the Arduino is connected to the laptop for monitoring the tracked vehicle’s speed. As is explained, the encoder is used to obtain a tracked vehicle’s speed. An important assumption is that the slip between the sprockets

and tracks can be neglected. As a result, the multiplication of the sprocket angular speed by its radius is equal to the tracked speeds. Therefore, this assumption is needed to deal with the complicated nature of this problem.

The next step is to find the speed correction factor, reported by the encoder on the monitor. There is a difference between the real speed and encoder reported speed because of noises.

For obtaining that factor, a series of experiments are conducted on two different surfaces. First, a specific distance is traveled at a constant speed reported by the encoder. Next, the real speed is obtained by dividing the distance length by the time. The results are reported in Table 3.

Table 3: Encoder speed vs. real speed in different surfaces

Surface type	Real speed (cm/s)	Speed recorded by the encoder (cm/s)
Wood	27.64	107
Carpet	28.73	108

The estimated mean correction factor is 0.26. Therefore, the speed reported on the monitor is acceptable.

The trafficability is tested for 13, 15, 20, 28 degrees with and without an arm. Both uphill and downhill trafficability is tested. Finally, the critical slope angle for tip-over the tracked vehicle with and without the arm is tested. Fig. 2 shows two instances of uphill and downhill experiments.



a



b

Fig. 2: Test instance; a) uphill test case; b) downhill test case

Table 4 summarizes the results of uphill tests without the arm.

Table 4: Results of uphill tests without arm

Slope (degree)	Start speed (cm/s)	Trafficability
13	22	Yes
15	22	Yes
20	22	Moving but there is high side slip, causes undesirable yaw angle
28	22	No (cannot pass the slope)

Table 5 summarizes the results of the downhill tilt tests without the arm.

Table 5: Results of the downhill tests without the arm

Slope (degree)	Start speed (cm/s)	Trafficability
13	22	Yes
15	22	Yes
20	22	Yes
28	22	Yes

Table 6 shows the results of the uphill tilt tests with the arm.

Table 6: Results of the uphill tests with the arm

Slope (degree)	Start speed (cm/s)	Trafficability
13	22	Yes
15	22	Yes
20	22	Moving but there is high side slip, causes undesirable yaw angle
28	22	No

Table 7 summarizes the results of the downhill tilt tests with the arm.

Table 7: Results of the downhill tests with the arm

Slope (degree)	Start speed (cm/Sec)	Trafficability
13	22	Yes
15	22	Yes
20	22	Yes
28	22	Yes

3.2 Experimental Results

1) The slope at 20 degrees is the test's critical slope. Although the tracked vehicle can traverse the slope, there is a high side slip, causes undesirable yaw angle.

2) The tracked vehicle can not pass the 28-degree slope. When it starts moving on the slope, slip increases to 100% and the tracks rolled in place.

Computer-aided simulations are used to carry out more tests. Experimental tests are more costly and time-consuming. Computer simulations allow the control of the model and the inclusion of non-linear terramechanics relationships, including track contact with soil.

4. Computer-aided Simulation

The RecurDyn is used to simulate the soil and multibody dynamic systems. The tracked vehicle, similar to the test samples, is designed. The RecurDyn is a computer-aided engineering software capable of simulating the multi-body dynamics. It can simulate both rigid and flexible body dynamics [27]. The tracked vehicle model simulated in the RecurDyn has a normal pressure equivalent to the original model (1.5 Kpa) and rubber tracks. The simulation goals are:

- ❖ Discovering the critical tip-over the slope
- ❖ Observing the impact of the tracked vehicle speed on the tip-over the slope.
- ❖ Finding the impact of the surface type (soil or rigid ground) on the tip- over the slope.

The tests are done with and without arm.

The arm moves the center of mass of the tracked vehicle moves the mass center. The aim

by adding t Fig. 3 shows the tracked vehicle model with and without the arm in RecurDyn. The normal pressure is 1.5 Kpa and arm was the dynamic evaluation of its effect on the tracked vehicle.

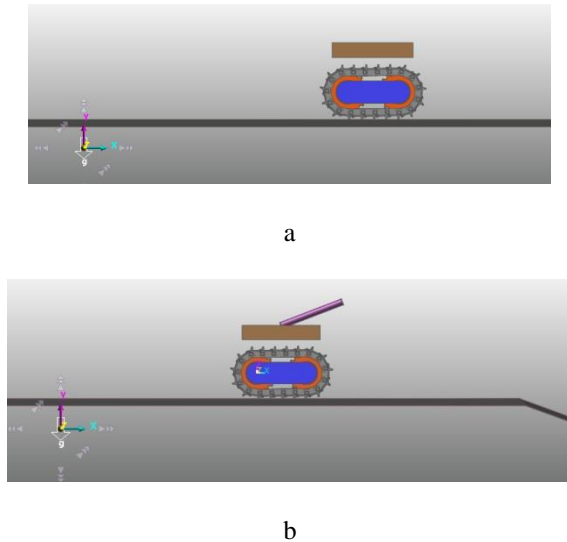


Fig. 3: Tracked vehicle model with and without arm in RecurDyn; a) tracked vehicle model in RecurDyn; b) tracked vehicle model with arm

The sample pathway is shown in Fig. 4. The simulation is done for three slope angles of 10, 15 and 20 degrees.



Fig. 4: Pathway sample model

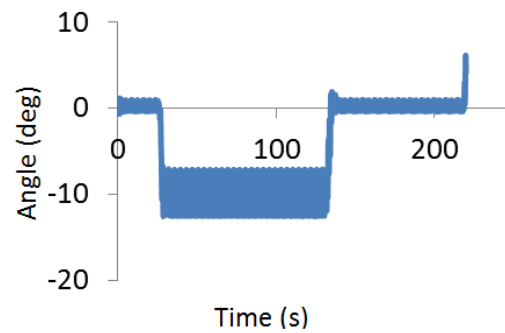
4.1 Results of Tracked Vehicle Model without Arm

In this part, the tracked vehicle is simulated without an arm.

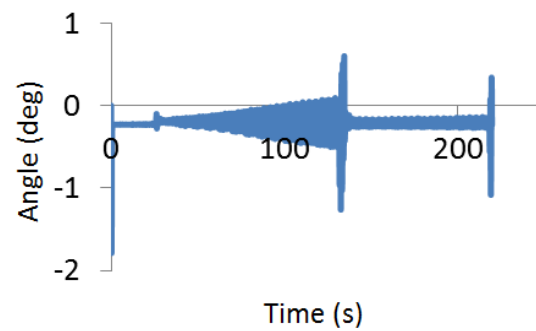
4.1.1 Constant Speed and Ground Type at Different Slopes

This level includes a rigid ground. The initial speed is constant for all steps while the slope changes. Figure 5 shows the pitch and roll angle of the tracked vehicle traversing on slope angles

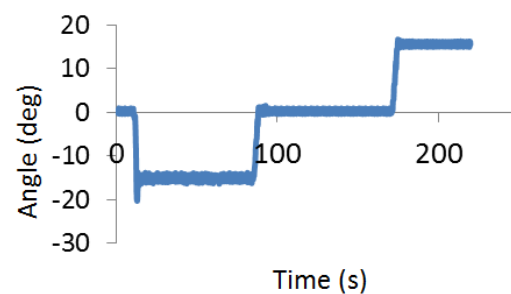
of 10 and 15 degrees. The tracked vehicle can pass both uphill and downhill slopes of 15 degrees. The tracked vehicle can not cross the 20-degree slope because of tip-over (Fig. 6).



a



b



c

Fuzzy Yaw Angle Controller for an Electric Tracked Vehicle

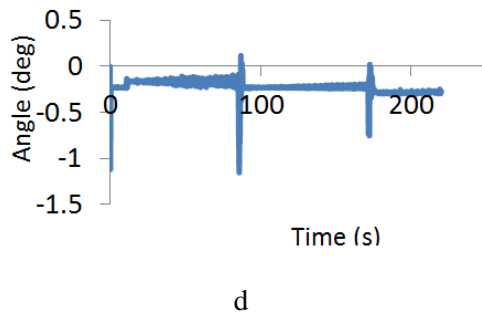


Fig. 5: Pitch and roll angle of the tracked vehicle in 10 and 15-degree slope pathway; a) pitch angle of the tracked vehicle in 10-degree slope pathway; b) roll angle of the tracked vehicle in 10-degree slope pathway; c) pitch angle of the tracked vehicle in 15-degree slope pathway; d) roll angle of the tracked vehicle in 15-degree slope pathway

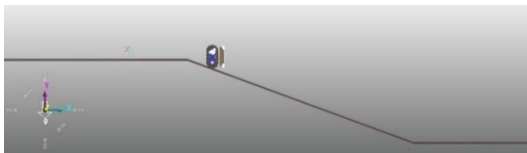
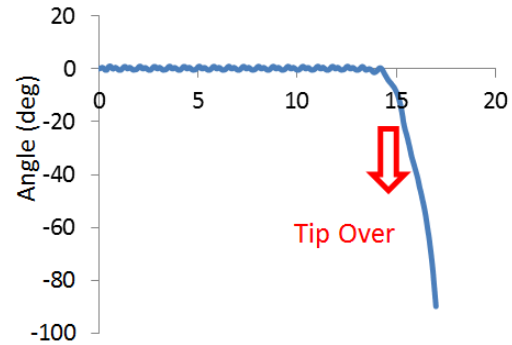


Fig. 6: Tip-over on 20-degree slope

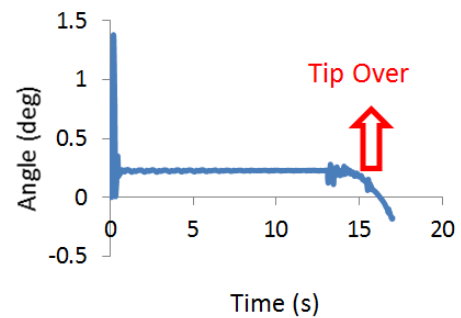
4.1.2 Constant Speed and Slope with Different Soil types

Speed is 22 cm/s and the slope is at 20 degrees, which is the critical slope. Rigid ground, dry sand, and sandy loam were tested.

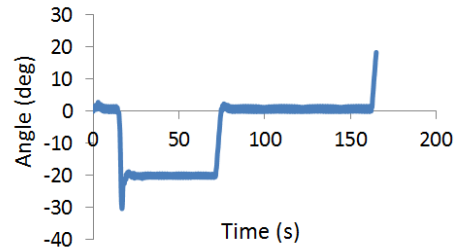
Fig. 7 shows the pitch and roll angle of the tracked vehicle on the rigid ground, dry sand and sandy loam. Tip-over is observed on the rigid ground and sandy loam (uphill). It can pass the sandy loam with a 20-degree downhill slope, but can not cross the 20-degree uphill slope.



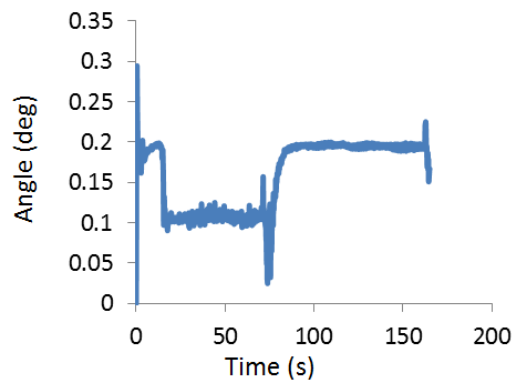
a



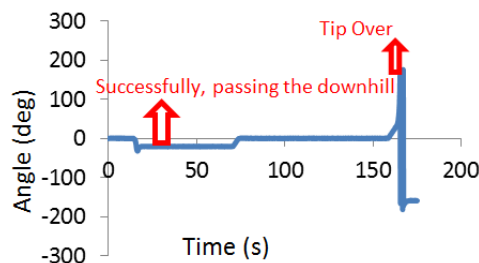
b



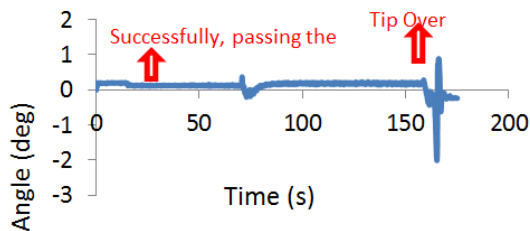
c



d



e



f

Fig. 7: Pitch and roll angle of the tracked vehicle on rigid ground, drysand and sandyloam; a) pitch angle of the tracked vehicle on rigid ground; b) roll angle of the tracked vehicle on rigid ground; c) pitch angle of the tracked vehicle on dry sand; d) roll angle of the tracked vehicle on dry sand; e) pitch angle of the tracked vehicle on sandy loam; f) roll angle of the tracked vehicle on sandy loam

This can be concluded that the soil type has a direct impact on the maximum possible gradient. The tracked vehicle can pass both 20-degree

uphill and downhill slopes with dry sand. In sandy loam, the tracked vehicle just can pass the downhill slope.

4.1.3 Constant Soil and Slope at Different Speeds

Here, slope and soil are considered to be constant. The slope of 20 degrees, which is the critical slope, and dry sandy soil are selected for experiments.

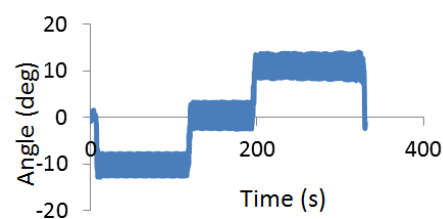
The model is tested at the speeds of 22, 27, 33, 38 and 44 cm/s. At the speed of 44 cm/s, tip-over is observed. This can be concluded that speed has a direct impact on the maximum possible gradient. The tracked vehicle's trafficability on the slope increases with reducing the speed.

4.2 Results of Tracked Vehicle with Arm

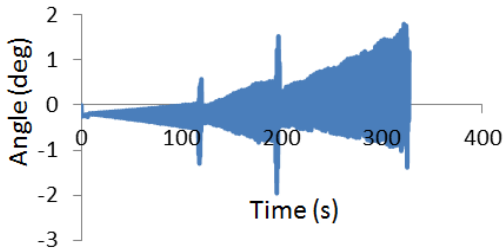
In this section, previous simulations are repeated for the tracked vehicle with the arm. The arm has a significant effect on the locomotion of the tracked vehicle.

4.2.1 Constant Speed and Ground Type and Different Slopes

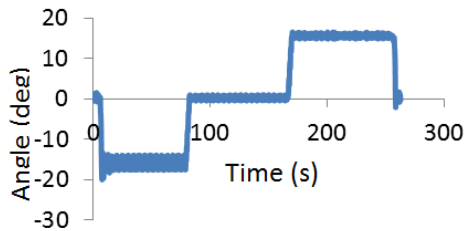
The experimental steps are precisely similar to the vehicle model without an arm. Fig. 8 respectively, shows the pitch angle of 10 degrees, the roll angle of 10 degrees, the pitch angle of 15-degrees and the roll angle of 15-degrees, respectively.



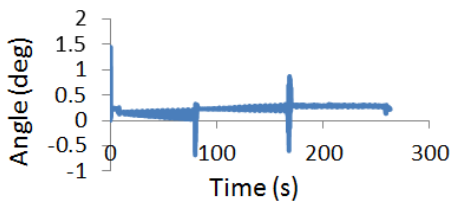
a



b



c



d

Fig. 8: Pitch and roll angle in 10 and 15 degree slope; a) pitch angle of the tracked vehicle with the arm in 10-degree slope; b) roll angle of the tracked vehicle with the arm in 10-degree slope; c) pitch angle of the tracked vehicle with the arm in 15-degree slope; d) roll angle of the tracked vehicle with the arm in 15-degree slope

The tracked vehicle with the arm can not move on a 20-degree slope. Figure 9 shows the occurred tip-over.

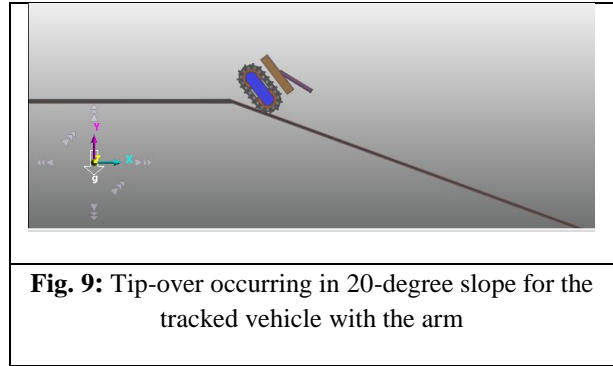


Fig. 9: Tip-over occurring in 20-degree slope for the tracked vehicle with the arm

4.2.2 Constant Speed and Slope constant and Different Soil Types

Unlike the tracked vehicle without an arm, changing the surface type does not improve the locomotion on the critical slope degree (20-degrees). Dry sand and sandy loam are tested and hanging over are observed in both of them.

5. Designing Yaw Controller for Straight Locomotion on Slopes

As was mentioned, a side slip was observed during slope-traversing, causing the formation of an undesirable yaw angle. In this section, three controlling systems are modeled for controlling the yaw angle of the tracked vehicle. The first system is a proposed yaw angle controller (PYAC). It uses a simple model as described by Wong [2] and a simple formulation for side-slip control. When the tracked vehicle slips to the right, the controller moves it to the left, and vice versa. This process is explained in detail in the PYAC section. The second system is a PI yaw angle controller (PIYC). The third one is a PID yaw angle controller (PIDYC). The fourth one is a fuzzy yaw angle controller (FYAC). Finally, the results from these four yaw angle controllers are compared.

5.1 Kinematics and Terramechanics Equations

When the tracked vehicle slips to the right, the controller moves it to the left, and vice versa. To

this end, it uses the tracked vehicle turning and steering equations [2].

$$R = \frac{B(r\omega_o + r\omega_i)}{2(r\omega_o - r\omega_i)} \quad (1)$$

Where, R is turning radius, B is the tread of the tracked vehicle (the spacing between the centerlines of the two tracks), ω_o and ω_i are, respectively, the outer and inner sprocket rotational speed, and r is sprocket radius. Different methods are employed for the tracked vehicle steering, such as skid steering, steering by articulation, and curved track steering [2]. The drawbar performance is an essential factor for off-road vehicle locomotion. It shows the ability of a vehicle to pull or push various types of working machinery. Drawbar pull F_d is the difference between the tractive effort F developed by running gear and the resultant resisting force $\sum R$ acting on the vehicle [2]:

$$F_d = F - \sum R \quad (2)$$

The resisting forces acting on an off-road vehicle include the internal resistance of the running gear, resistance due to vehicle-terrain interaction, obstacle resistance, grade resistance, and aerodynamic drag [2]. The thrust of the outside and inside tracks, the resultant resisting force, the moment of turning resistance acting on the track by the ground, and vehicle parameters affect the turning behavior of a tracked vehicle using skid-steering [2]. The motion resistance (R_c) against pressing the terrain by a track is expressed by [28]:

$$R_c = \frac{1}{(n+1)b^n \left(\frac{k_c}{b} + k_\phi\right)^{\frac{1}{n}}} \left(\frac{W}{l}\right)^{(n+1)/n} \quad (3)$$

Where W is the weight of the tracked vehicle, n is the exponent of sinkage, b is the width of a track, k_c is the cohesive modulus, l is the length of the track, and k_ϕ is the frictional modulus.

The second term of $\sum R$ is $(\pm)W\sin(\alpha)$ which α is the slope angle [29]. A negative sign is for the time when the small tracked vehicle goes downhill and vice versa.

The thrust can be calculated by [2]:

$$F = \frac{M\varepsilon_o\eta_t}{r} \quad (4)$$

Where M is the motor output torque, ε_o is the overall reduction ratio of the transmission, η_t is overall transmission efficiency, r is the radius of the sprocket.

The maximum thrust capacity can be predicted by [5]:

$$F_{max} = cA + W\tan\Phi \quad (5)$$

Where, A is track area, c is cohesion, Φ is the angle of shearing resistance. Motion resistance is the most important resistance force during motion [30]. The mentioned equations are the basis of the experimental and simulation work.

5.2 Proposed Yaw Angle Controller (PYAC)

The initial rotational speed of sprockets is 0.8 rad/s. For controlling the yaw angle by keeping it zero and straight locomotion on the slope, the following controlling algorithm is defined: If the yaw angle is zero, then both right and left sprocket rotational speeds would be 0.8 rad/s, else if there as a positive yaw angle, the right and left sprocket rotational speeds would be, respectively, 0.6 and 0.8 rad/s, else the right and left sprocket rotational speeds would be 0.8 and 0.6 rad/s, respectively.

Fig. 10 shows the controlling model by linking Matlab Simulink and RecurDyn. The yaw angle

Fuzzy Yaw Angle Controller for an Electric Tracked Vehicle

is the RecurDyn output under the mentioned scenario. Right and left rotational sprocket speeds are the inputs of the RecurDyn block.

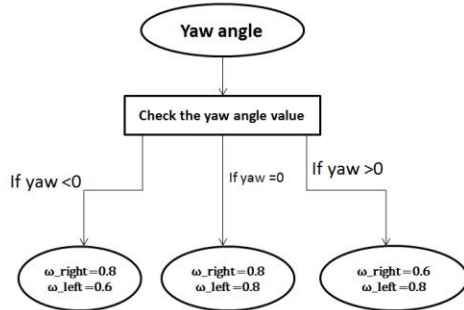


Fig. 10: The controlling model by linking Matlab Simulink and RecurDyn

5.3 PI Yaw Angle Controller (PIYC)

After completing several simulations and repetitions, the best possible system numbers are finally obtained. When P is too high (e.g. P=10), the sensitivity of the system to the slope and yaw angle reverses the direction of movement of the sprockets. It inhibits slope-traversing by reversing the tracked vehicle after entering the slope. If I exceed 1.5, the sensitivity will increase and the controlling system would reverse the small tracked vehicle, inhibiting slope-traversing. The best possible value for P is between 0.1 to 0.2 and for I is 1.5.

5.4 PID Yaw Angle Controller (PIDYC)

The description of the previous section also applies to this section, except that after some trials the best values for D and N are 2 and 10, respectively. Fig. 11 shows the PI Yaw Angle Controller and PID Yaw Angle Controller systems. Although both systems have similar co-simulation models, D was zero in the PI system.

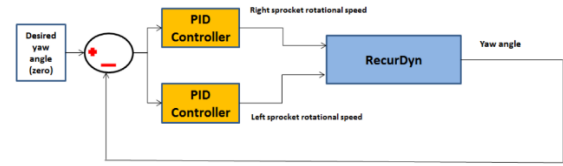


Fig. 11: PI and PID yaw angle controller models

5.5 Fuzzy Yaw Angle Controller (FYAC)

The fuzzy yaw angle controller is designed in this section. The input is the yaw angle of the small tracked vehicle and the outputs are the right and left sprocket rotational speeds. Fig. 12 shows the fuzzy yaw angle controller model.

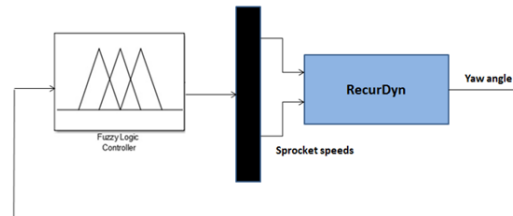
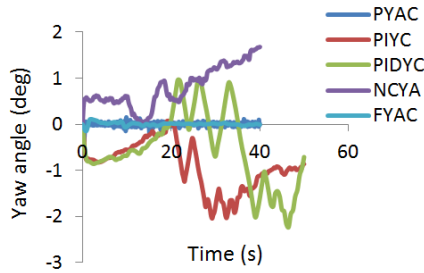


Fig. 12: Fuzzy yaw angle controller

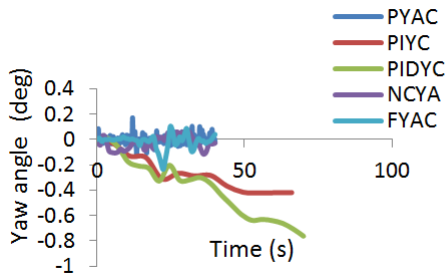
5.6 Co-Simulation Results

Simulations are done for three types of terrain, namely rigid ground, dry sand, and sandy loam. These results are compared to the results from four controllers.

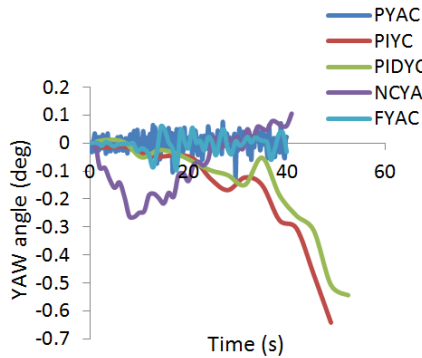
The results of the not controlled yaw angle (NCYA) are also presented. Fig. 13 shows the co-simulation results.



a



b

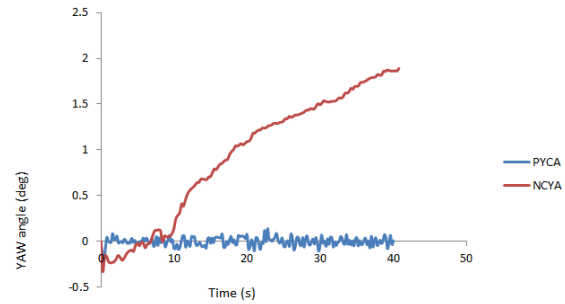


c

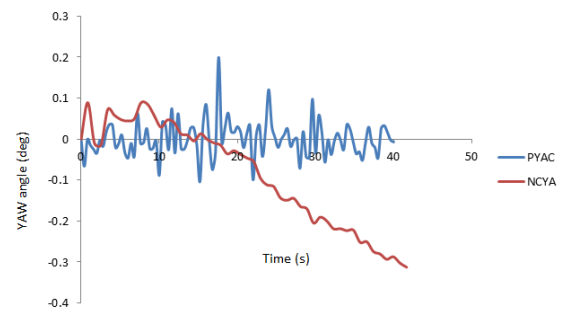
Fig. 13: Co-simulation results; a) rigid ground; b) dry sand; c) sandy loam

It is evident that the PYAC has the fastest response as compared to the PIYC and PIDYC. It helps the tracked vehicle have a straight slope-traversing. PIYC and PIDYC take longer to traverse the same distance than the PYAC.

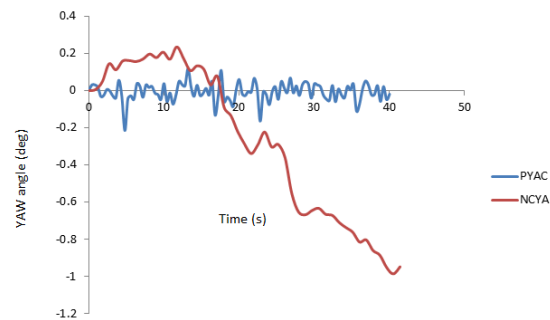
PYAC performs better in maintaining a zero yaw angle during slope-traversing. FYAC has a smoother response than PYAC. As PYAC has a more straightforward structure and regulations, the co-simulation of the small tracked vehicle with the arm has done by it. Fig. 14 shows the co-simulation results of a small tracked vehicle with the arm and desirable results are obtained.



a



b



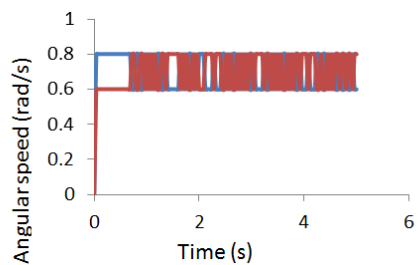
c

Fig. 14: Co-simulation results of the small tracked vehicle with arm; a) rigid ground; b) dry sand c)

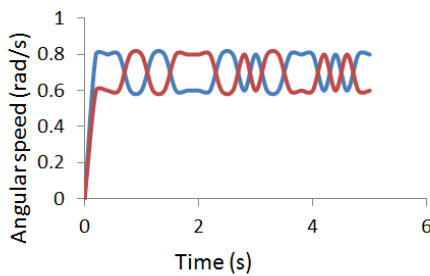
sandy loam

vehicle with the arm (rad/s)

The locomotion of the small tracked vehicle with the PYAC is desirable. Fig. 15 shows the sprocket rotational speeds (rad/s) on a rigid ground, which is selected as a sample ground based on the proposed yaw angle controlling algorithm for the tracked vehicle with and without the arm for first a five-second simulation. This algorithm continues during the whole simulation time. In all figures, the red and blue lines stand for the left and right rotational sprocket speeds, respectively.



a



b

Fig. 15: The instance sprocket rotational speeds (rad/s) which have been selected based on the proposed yaw angle controlling algorithm on rigid ground; a) the sprocket rotational speeds selected by controlling algorithm for the tracked vehicle without the arm (rad/s); b) the sprocket rotational speeds selected by controlling algorithm for the tracked

The pitch angle is verified with [31]. The yaw angle has been verified by [32] and in both cases, the mean error is less than 10%.

6. Conclusion

The experimental trafficability test is applied to a small tracked vehicle traversing on a slope. The pitch and yaw angles are examined using the slope-traversing test. As the angle of inclination increases, An undesirable yaw angle is observed with increasing the inclination until a tip-over occurred. RecurDyn is used to simulate and model the tracked vehicle traversing on soils with different terramechanics characteristics (such as rigid ground, dry sand, and sandy loam) to evaluate the performance of the vehicle trafficability on a slope. The effect of soil and the tracked vehicle speed on slope-traversing is studied. In some cases, changing the type of soil allows for locomotion. In experimental tests, an undesirable yaw angle is observed in the 20-degree slope. The proposed yaw angle control system is designed for controlling the yaw angle of the tracked vehicle. It is then compared to the PI, PID, and fuzzy yaw angle controllers. The PYAC shows the best results as compared to the PI and PID yaw angle controllers. It is also faster and more accurate than PI and PID controllers. It maintained the tracked vehicle at zero yaw angle for straight slope-traversing. PYAC and FYAC both of them have almost similar results. FYAC has a faster response but PYAC has a slightly simpler structure. All controllers are designed based on the co-simulation of MATLAB Simulink and the RecurDyn.

- Developing an experimental off-road laboratory

- Finding the critical angles, such as tip-over and undesirable yaw, of small tracked vehicles for slope-traversing
- Designing a yaw angle controller for the tracked vehicle by co-simulation between MATLAB Simulink and RecurDyn.

Studying the rotational motion and designing an advanced controller can be a useful research field for future work.

References

- [1] S. A. A. Moosavian and A. Kalantari, "Experimental slip estimation for exact kinematics modeling and control of a Tracked Mobile Robot". *2008 IEEE/RSJ International conference on intelligent robots and systems*, Nice, France, pp. 95–100, (2008).
- [2] J. Y. (Jo Y. Wong), *Theory of ground vehicles*. Wiley, (2008).
- [3] N. Babu, S. Sujatha, S. Narayanan, and V. Balamurugan, "New approach for prediction of influence of vehicle dynamics parameters on instability of unmanned track vehicle using robotic approach," *Journal of mechanical science and technology*, vol. 32, no. 3, pp. 1357–1365, (2018).
<https://link.springer.com/article/10.1007/s12206-018-0239-0>
- [4] M. Bekker, "Introduction to terrain-vehicle systems," University of Michigan Press, (1969).
- [5] J. Y. Wong, *Terramechanics and off-road vehicle engineering: terrain behaviour, off-road vehicle performance and design*, Butterworth-Heinemann, (2009).
- [6] G. Yamauchi, D. Suzuki, and K. Nagatani, "Online slip parameter estimation for tracked vehicle odometry on loose slope". *SSRR 2016 – International symposium on safety, security, and rescue robotics*, Lausanne, Switzerland, pp. 227–232, (2016).
- [7] W. Wang, Z. Yan, and Z. Du, "Experimental study of a tracked mobile robot's mobility performance", *Journal of terramechanics*, vol. 77, pp. 75–84, (2018).
<https://www.sciencedirect.com/science/article/abs/pii/S0022489818300624>
- [8] M. Wang, C. Wu, T. Ge, Z. M. Gu, and Y. H. Sun, "Modeling, calibration and validation of tractive performance for seafloor tracked trencher", *Journal of terramechanics*, vol. 66, pp. 13–25, (2016).
<https://www.sciencedirect.com/science/article/abs/pii/S0022489816000227>
- [9] H.-W. Kim, S. Hong, J. Choi, and T. H. Lee, "An Experimental Study On Tractive Performance of Tracked Vehicle On Cohesive Soft Soil". *Fifth ISOPE Ocean Mining Symposium*, Japan, (2003).
- [10] E. Schulte, R. Handschuh, and W. Schwarz, "Transferability of Soil Mechanical Parameters to Traction Potential Calculation of a Tracked Vehicle". *Fifth ISOPE Ocean Mining Symposium*, Japan, (2003).
- [11] S. H. Baek, G. B. Shin, C. K. Chung, "Assessment of the side thrust for off-road tracked vehicles based on punching shear theory", *Journal of terramechanics*, vol. 79, pp. 59-68, (2018).
<https://www.sciencedirect.com/science/article/abs/pii/S0022489817302306>
- [12] A. Gallina, R. Krenn, and B. Schäfer, "On the treatment of soft soil parameter uncertainties in planetary rover mobility

simulations”, *Journal of terramechanics*, vol. 63, pp. 33–47, (2016).

<https://www.sciencedirect.com/science/article/abs/pii/S0022489815000725>

[13] T. Zou, J. Angeles, and F. Hassani, “Dynamic modeling and trajectory tracking control of unmanned tracked vehicles”, *Robotics and autonomous systems*, vol. 110, pp. 102–111, (2018).

<https://www.sciencedirect.com/science/article/pii/S0921889018300319>

[14] S. Tang, S. Yuan, J. Hu, X. Li, J. Zhou, and J. Guo, “Modeling of steady-state performance of skid-steering for high-speed tracked vehicles”, *Journal of terramechanics*, vol. 73, pp. 25–35, (2017).

<https://www.sciencedirect.com/science/article/abs/pii/S0022489817300757>

[15] M. Ahmadi, V. Polotski, and R. Hurteau, “Path tracking control of tracked vehicles”. *Proceedings-IEEE Proceedings 2000 ICRA. Millennium Conference. IEEE International Conference on Robotics and Automation. Symposia Proceedings (Cat. No.00CH37065)*, USA, pp. 2938–2943, (2000).

[16] Y. Dai, X. Zhu, H. Zhou, Z. Mao, and W. Wu, “Trajectory tracking control for seafloor tracked vehicle by adaptive neural-fuzzy inference system algorithm”, *International journal of computers communications and control*, vol. 13, no. 4, pp. 465–476, (2018).

<http://univagora.ro/jour/index.php/ijccc/article/view/3267>

[17] B. Janarthanan, C. Padmanabhan, and C. Sujatha, “Lateral dynamics of single unit skid-steered tracked vehicle”, *International journal of automotive technology*, vol. 12, no. 6, pp. 865–875, (2011).

<https://link.springer.com/article/10.1007/s12239-011-0099-4>

[18] Q. Ye, R. Wang, Y. Cai, X. Xu, X. Meng, and C. Long, “A study of the novel vision guided IV trajectory tracking control system based on expected yaw velocity”, *Advances in engineering software*, vol. 131, pp. 196–204, (2019).

<https://www.sciencedirect.com/science/article/pii/S0965997817306221>

[19] X. Xu, L. Zhang, Y. Jiang, and N. Chen, “Active Control on Path Following and Lateral Stability for Truck–Trailer Combinations”, *Arabian journal for science and engineering*, vol. 44, no. 2, pp. 1365–1377, (2019).

<https://link.springer.com/article/10.1007/s13369-018-3527-1>

[20] J. Cai, H. Jiang, L. Chen, J. Liu, Y. Cai, and J. Wang, “Implementation and Development of a Trajectory Tracking Control System for Intelligent Vehicle”, *Journal of intelligent & robotic systems*, vol. 94, no. 1, pp. 251–264, (2019).

<https://link.springer.com/article/10.1007/s10846-018-0834-4>

[21] X. J. Jin, G. Yin, X. Zeng, and J. Chen, “Robust gain-scheduled output feedback yaw stability control for in-wheel-motor-driven electric vehicles with external yaw-moment”, *Journal of the Franklin institute*, vol. 355, no. 18, pp. 9271–9297, (2018).

<https://www.sciencedirect.com/science/article/pii/S0016003217303204>

[22] M. Jiang, Y. Dai, L. Cui, and B. Xi, “Experimental and DEM analyses on wheel-soil interaction”, *Journal of terramechanics*, vol. 76, pp. 15–28, (2018).

<https://www.sciencedirect.com/science/article/abs/pii/S0022489817300290>

[23] Power, “Specifications.”, <http://www.sunnybatt.com/pdf/SLA/SB/12/SB1229.pdf>

[24] Dayuse, “About us,” 2017. [Online]. Available: <https://www.dayuse.com/pages/dayuse/company>

[25] “Getting Started with Arduino and Genuino products,” 2019. [Online]. Available: <https://www.arduino.cc/en/Guide/HomePage>.

[26] N. A. A. M. Nasir, M. N. Mohtar, and N. A. M. Yunus, “Development of Signal Generator for Lab on a Chip Application”. *2018 IEEE 5th International Conference on Smart Instrumentation, Measurement and Application (ICSIMA)*, Songkla, Thailand, pp. 1–4, (2018).

[27] “RecurDyn | Multi-Body Dynamics CAE.” [Online]. Available: <https://functionbay.com/en/page/single/2/recurdyn-overview>. [Accessed: 10-May-2019].

[28] G. Mastinu, M. Ploechl, and M. Ploechl, *Road and Off-Road Vehicle System Dynamics Handbook*. CRC Press, (2013).

[29] B. Mashadi and D. Crolla, *Vehicle Powertrain Systems*. Wiley, (2011).

[30] M. Masih-Tehrani and S. Ebrahimi-Nejad, “Hybrid Genetic Algorithm and Linear Programming for Bulldozer Emissions and Fuel-Consumption Management Using Continuously Variable Transmission”, *Journal of construction engineering and management*, vol. 144, no. 7, (2018).

<https://ascelibrary.org/doi/abs/10.1061/%28ASCE%29CO.1943-7862.0001490>

[31] S. B. Choi, D. W. Park, and M. S. Suh, “Fuzzy sky-ground hook control of a tracked vehicle featuring semi-active electrorheological suspension units,” *J. Dyn. Syst. Meas. Control. Trans. ASME*, vol. 124, no. 1, pp. 150–157, 2002.

[32] K. Nam, S. Oh, H. Fujimoto, and Y. Hori, “Design of adaptive sliding mode controller for robust yaw stabilization of in-wheel-motor-driven electric vehicles,” 2012.